CHAPTER IV
RESULTS AND DISCUSSION

4.1 Dynamic Adsorption: Multi-Component Pulse Test

The C_8 aromatics were adsorbed on the zeolites in the column and continuously desorbed by the desorbent stream, toluene. Concentration of each species in the effluent was plotted versus effluent volume as shown in Figures 4.1-4.10. n-C_9 is used as a tracer or reference component because it can not be adsorbed in the zeolite pore. Therefore, retention volume of the tracer corresponds to the void volume in the column. By using the ratio of the net retention volume of *p*-xylene to the net retention volume of other C_8 aromatics, *p*-xylene selectivity with respect to other components were calculated. The results are shown in Tables 4.1 and 4.2.

Figures 4.11 and 4.12 show the correlation plot between *p*-xylene selectivity, zeolite acidity and cationic radius of *X* and *Y* zeolites, respectively. The intermediate electronegativity of a substance, S_{int}, represents the acidity of an adsorbent. The higher the S_{int}, the higher the acidity. For both *X* and *Y* zeolites, the acidity increases as *Cs, Rb, K, Na* and *Li* exchanged zeolites whereas the ionic radius decreases as *Cs, Rb, K, Na* and *Li*. If the adsorption mechanism of the C_8 aromatics were solely restricted by the acid-base interaction, the selectivity of *p*-xylene, which is the least basic xylene, would decrease with increasing the zeolite acidity. In other words, the selectivity would decrease in the order of *Cs, Rb, K, Na* and *Li* exchanged zeolites. However, the results on the *X* and *Y* zeolites show that the *p*-xylene selectivity with respect to *o*-xylene increases from *Cs* to *Rb* and *K*, then decreases from *K* to *Na* and *Li* exchanged zeolites. The same trend can be seen on the *p*-xylene selectivity with respect to *m*-xylene of the exchanged *X* zeolites. For the *p*-xylene selectivity with respect to *m*-xylene of *Y* zeolites, the trend is similar except that the selectivity slightly increases from *Na* to *Li* exchanged *Y* zeolites. These phenomena are probably contributed from both the exchanged cation size and acid-base interaction. For the first three exchanged cations, *Cs, Rb* and *K*, the effect of the exchanged cation on the selectivity is more pronounced. The orientation of *p*-xylene

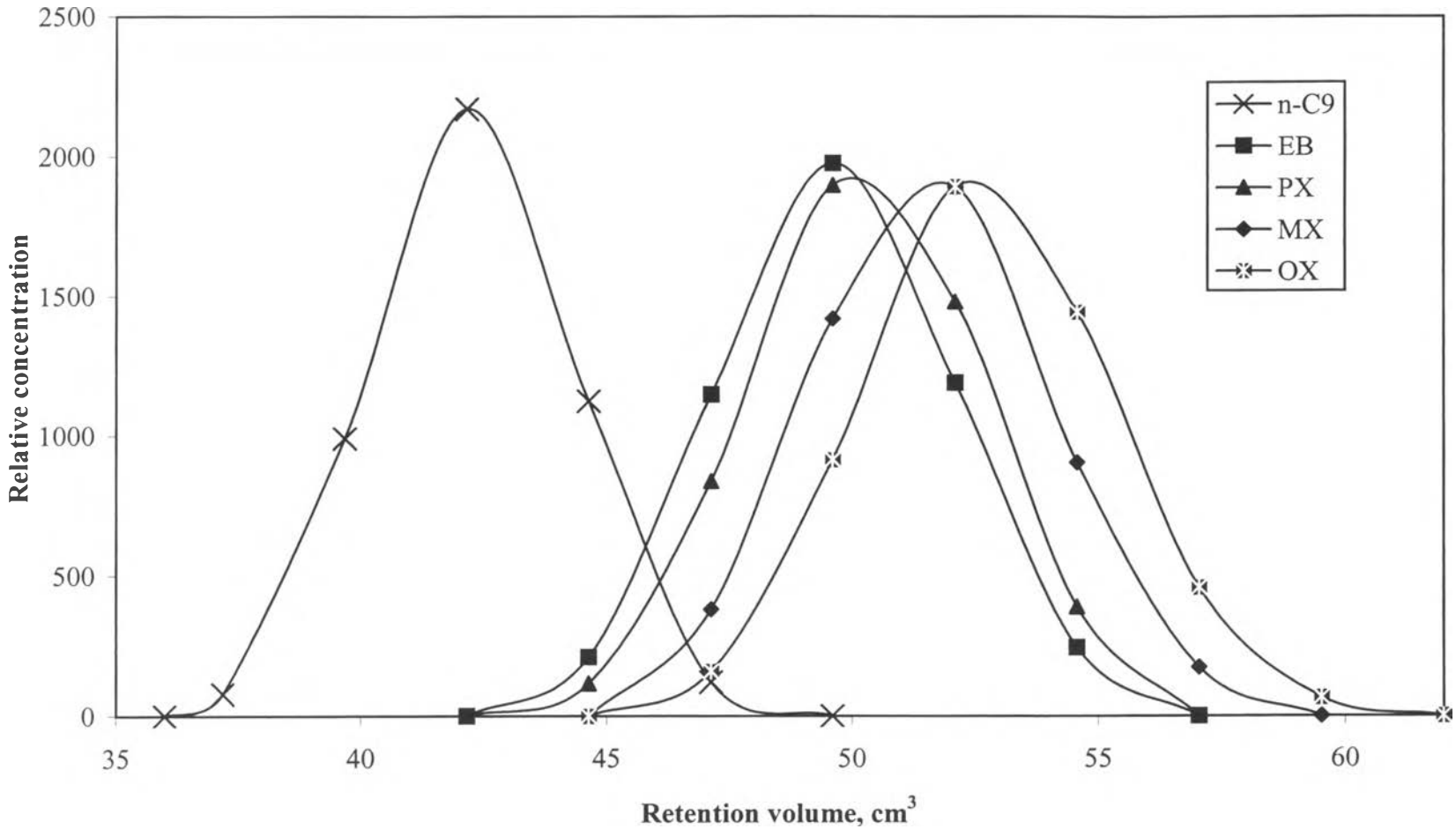

Figure 4.1 Dynamic adsorption: Multi-component pulse test on *LiX*

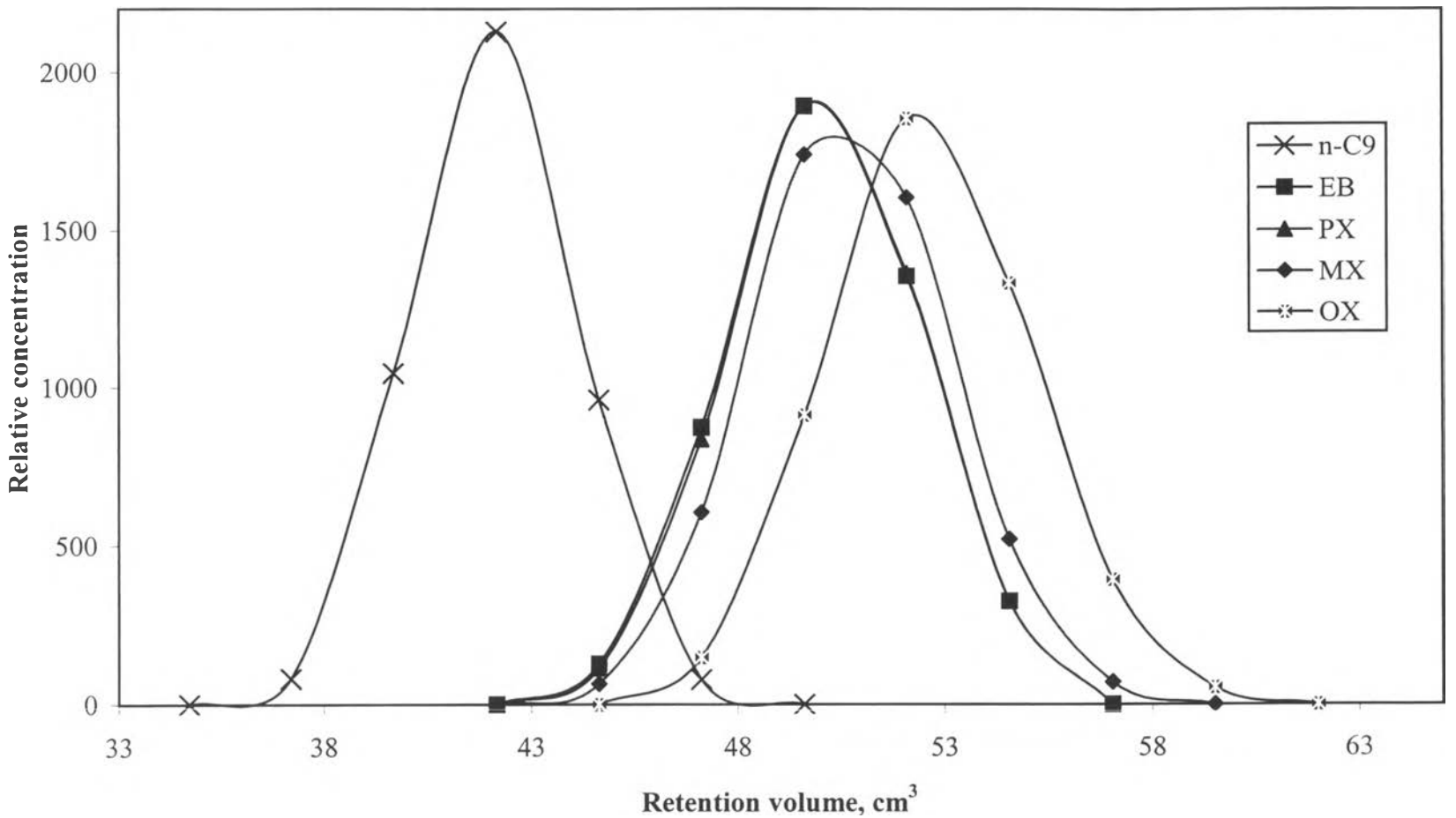

Figure 4.2 Dynamic adsorption: Multi-component pulse test on *NaX*

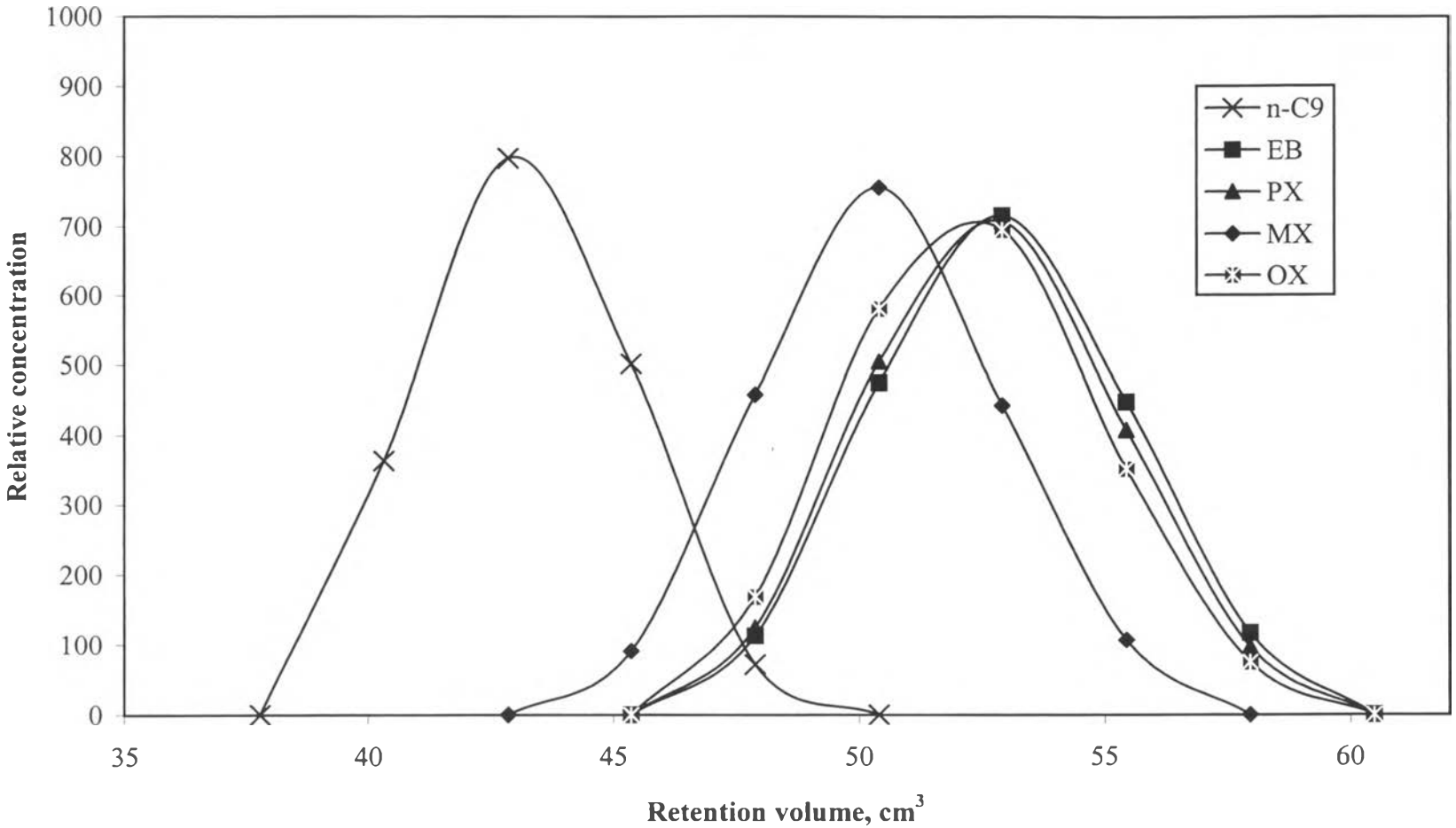

Figure 4.3 Dynamic adsorption: Multi-component pulse test on *KX*

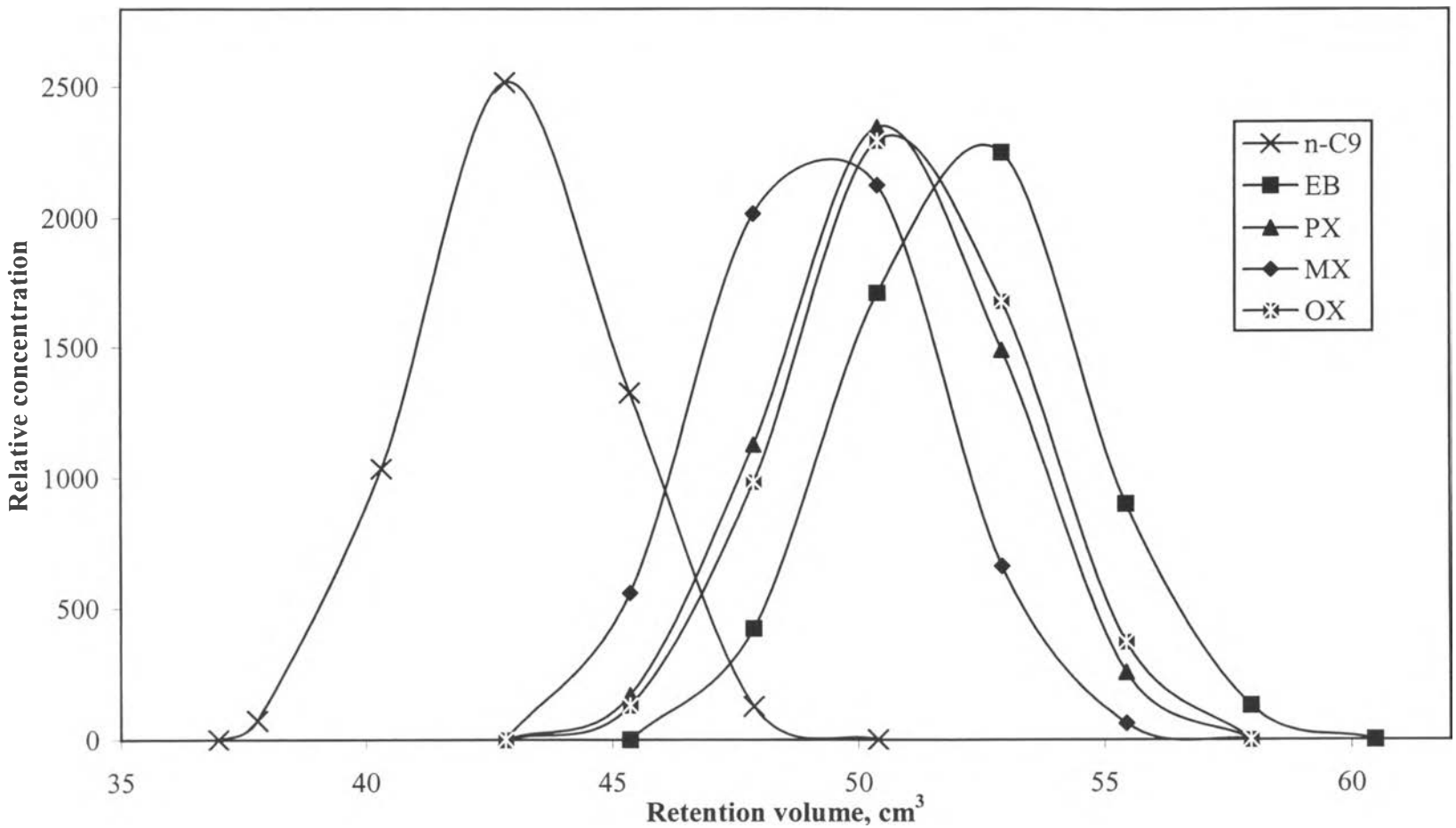

Figure 4.4 Dynamic adsorption: Multi-component pulse test on *RbX*

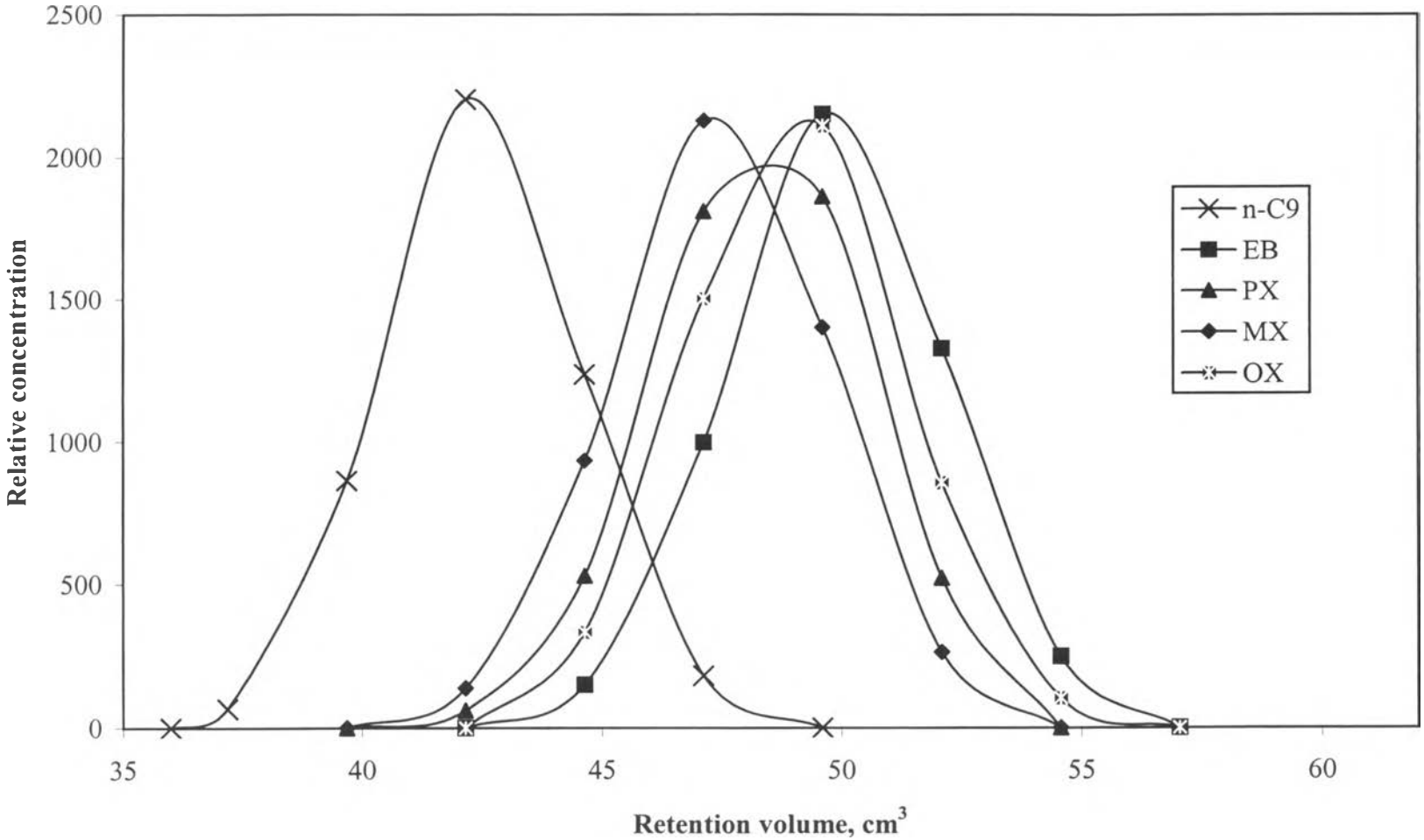

Figure 4.5 Dynamic adsorption: Multi-component pulse test on *CsX*

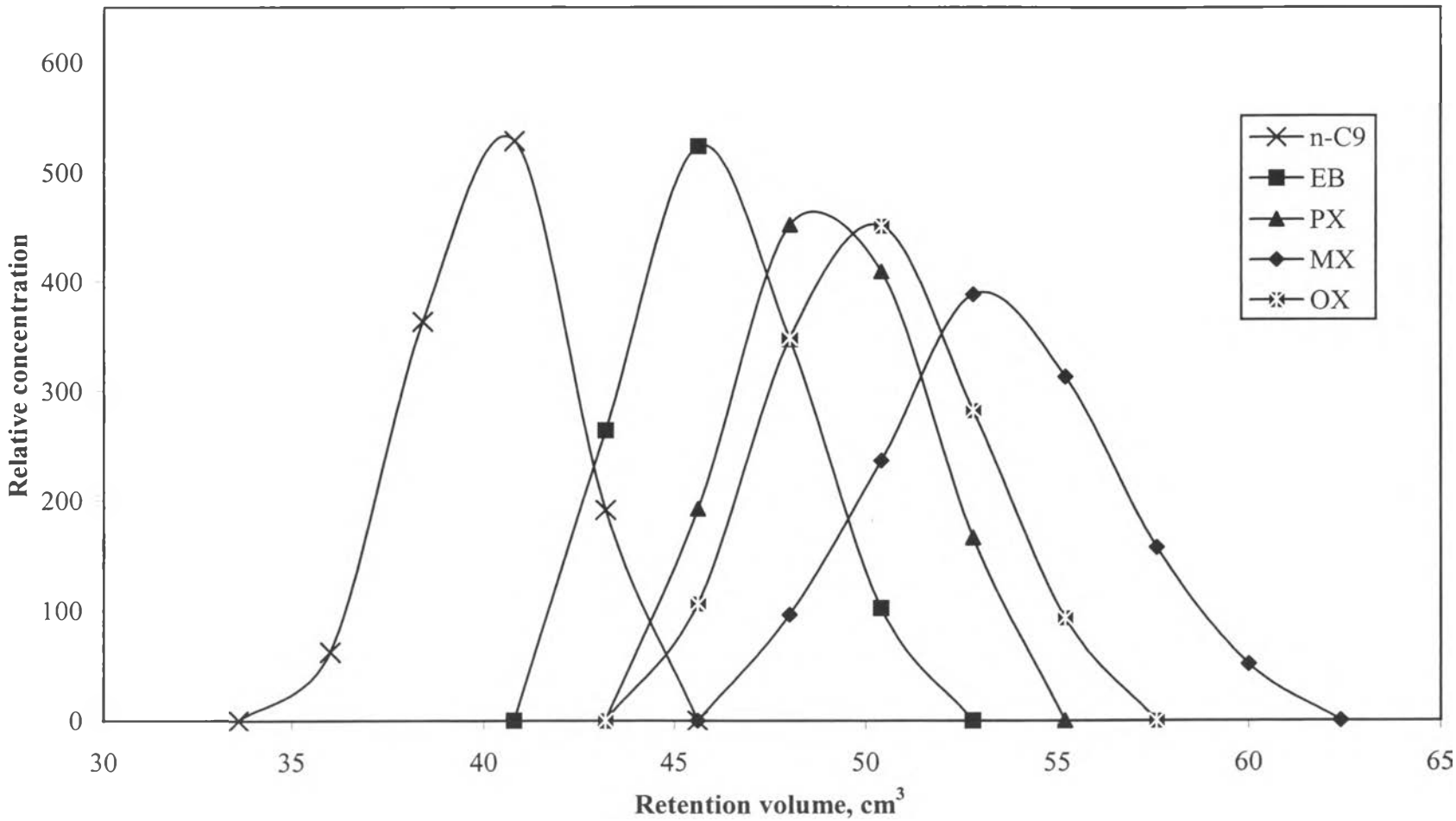

Figure 4.6 Dynamic adsorption: Multi-component pulse test on *LiY*

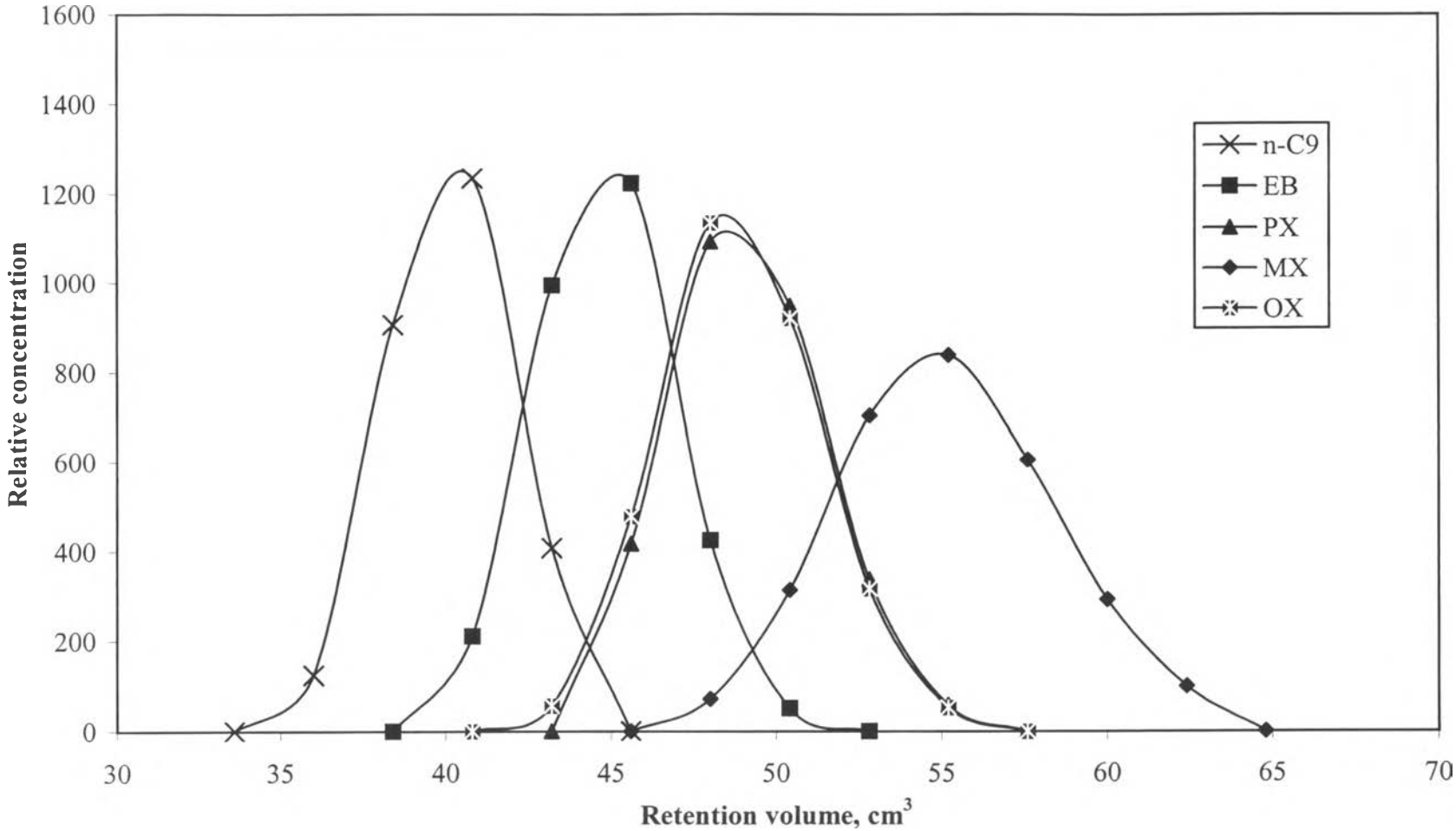

Figure 4.7 Dynamic adsorption: Multi-component pulse test on *NaY*

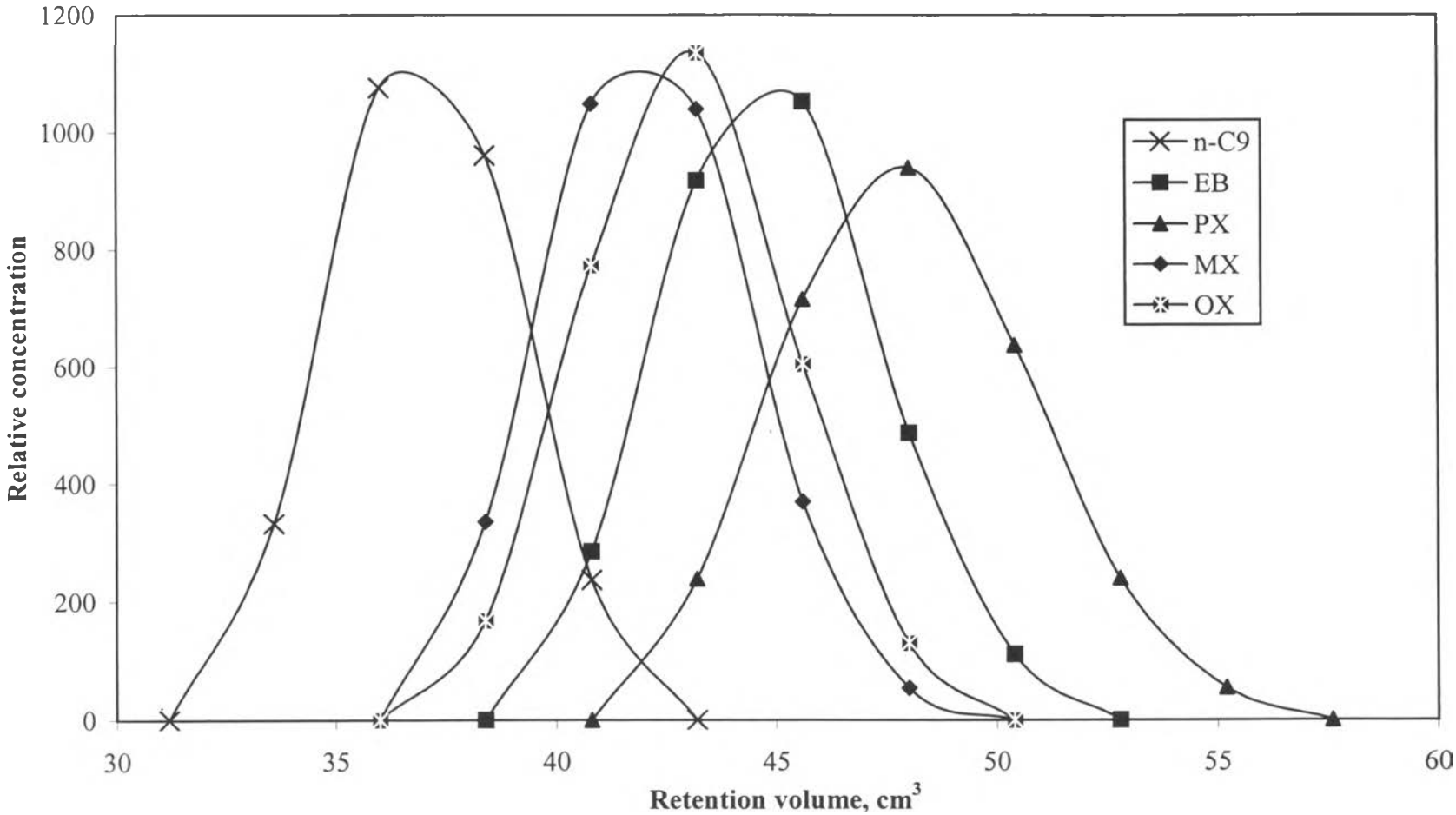

Figure 4.8 Dynamic adsorption: Multi-component pulse test on *KY*

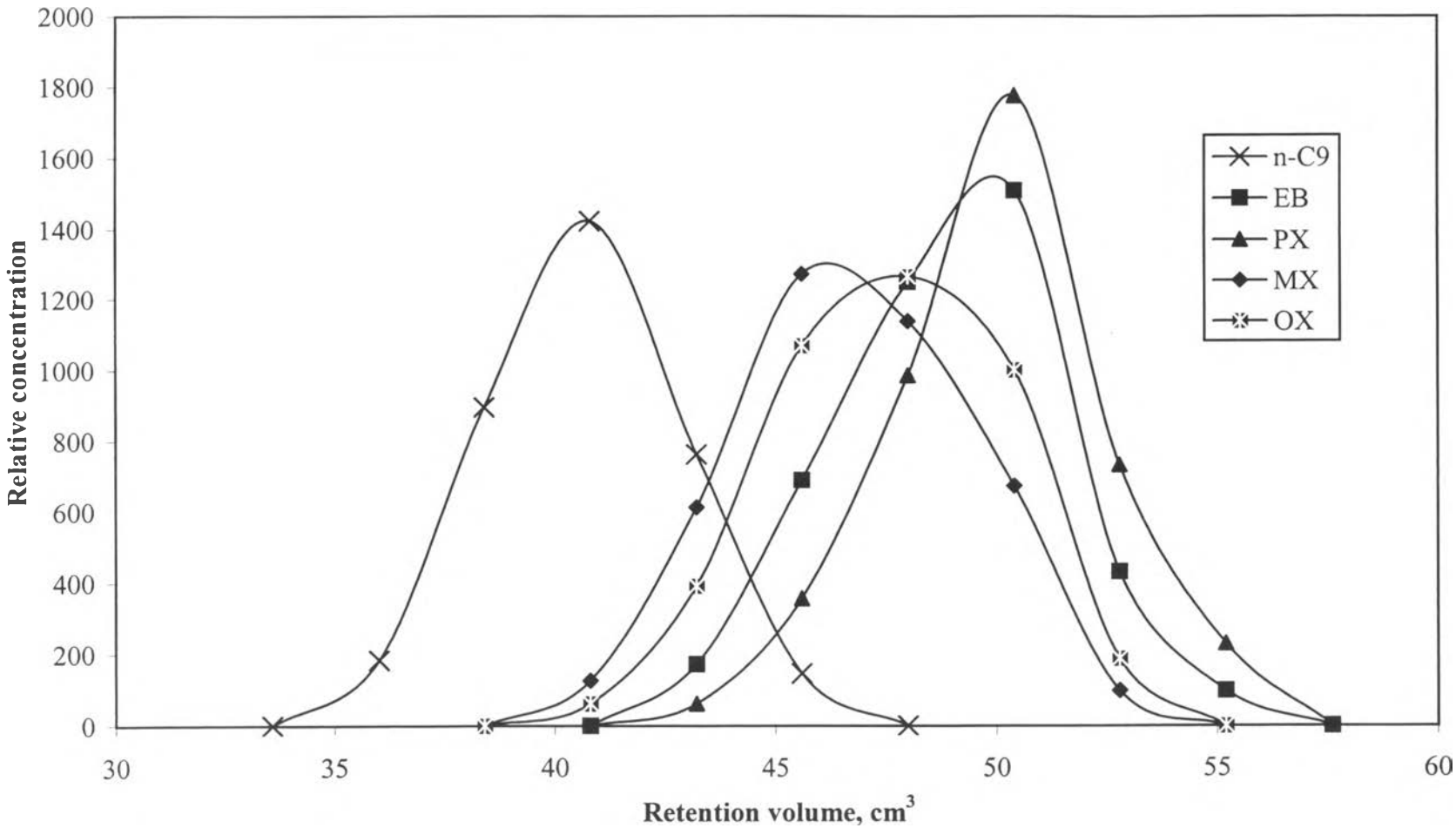

Figure 4.9 Dynamic adsorption: Multi-component pulse test on *RbY*

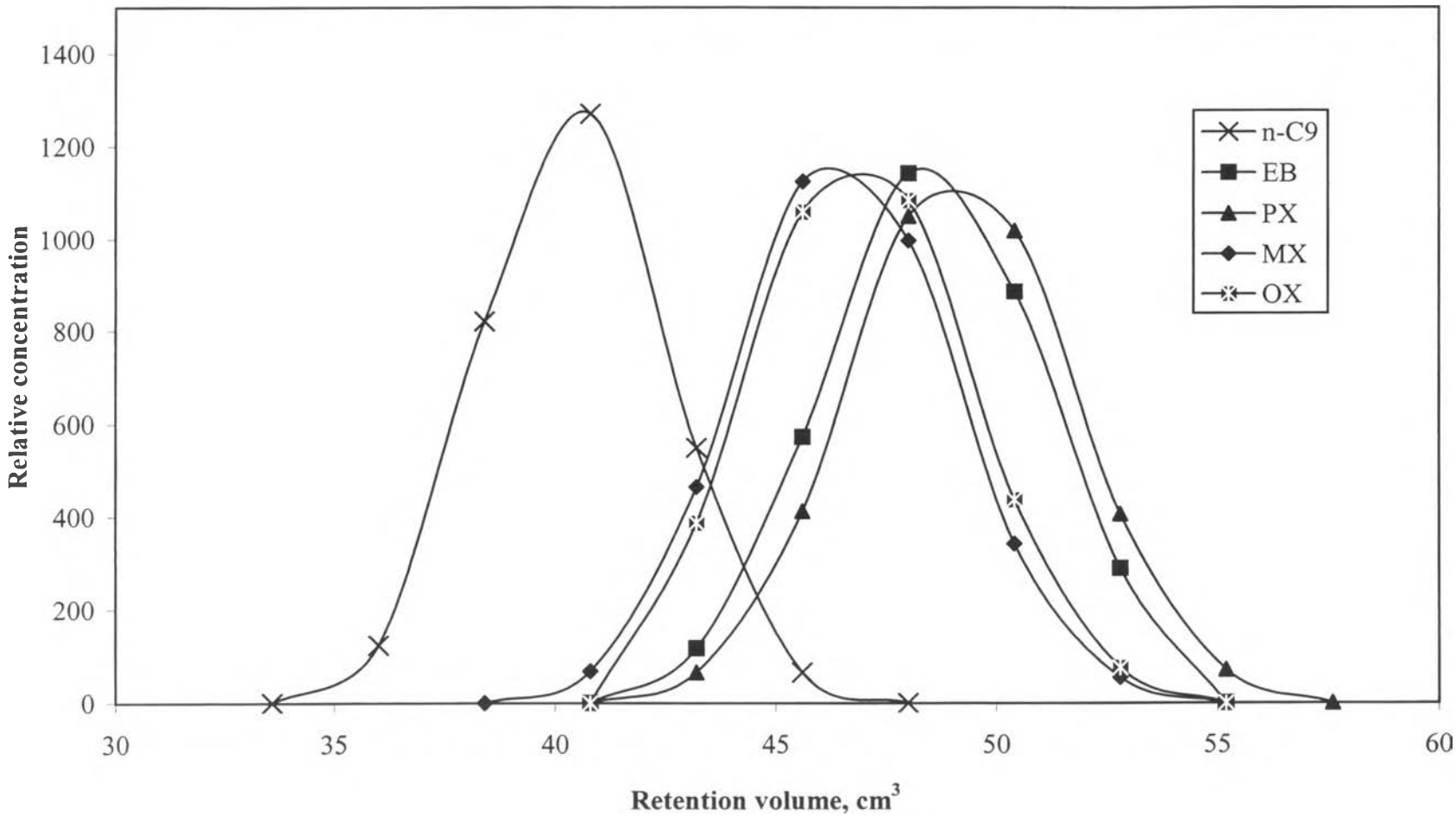

Figure 4.10 Dynamic adsorption: Multi-component pulse test on *CsY*

Table 4.1 *p*-xylene selectivity with respect to the other components of *X* zeolites

X zeolites	PX/EB	PX/OX.	PX/MX
LiX	1.097	0.761	0.856
NaX	1.321	0.761	0.930
KX	0.980	1.040	1.315
RbX	0.825	0.962	1.218
CsX	0.787	0.888	1.163

Table 4.2 *p*-xylene selectivity with respect to the other components of *Y* zeolites

Y zeolites	PX/EB	PX/OX.	PX/MX
LiY	1.503	0.884	0.668
NaY	1.907	1.024	0.597
KY	1.394	1.844	2.156
RbY	1.130	1.351	1.534
CsY	1.086	1.340	1.428

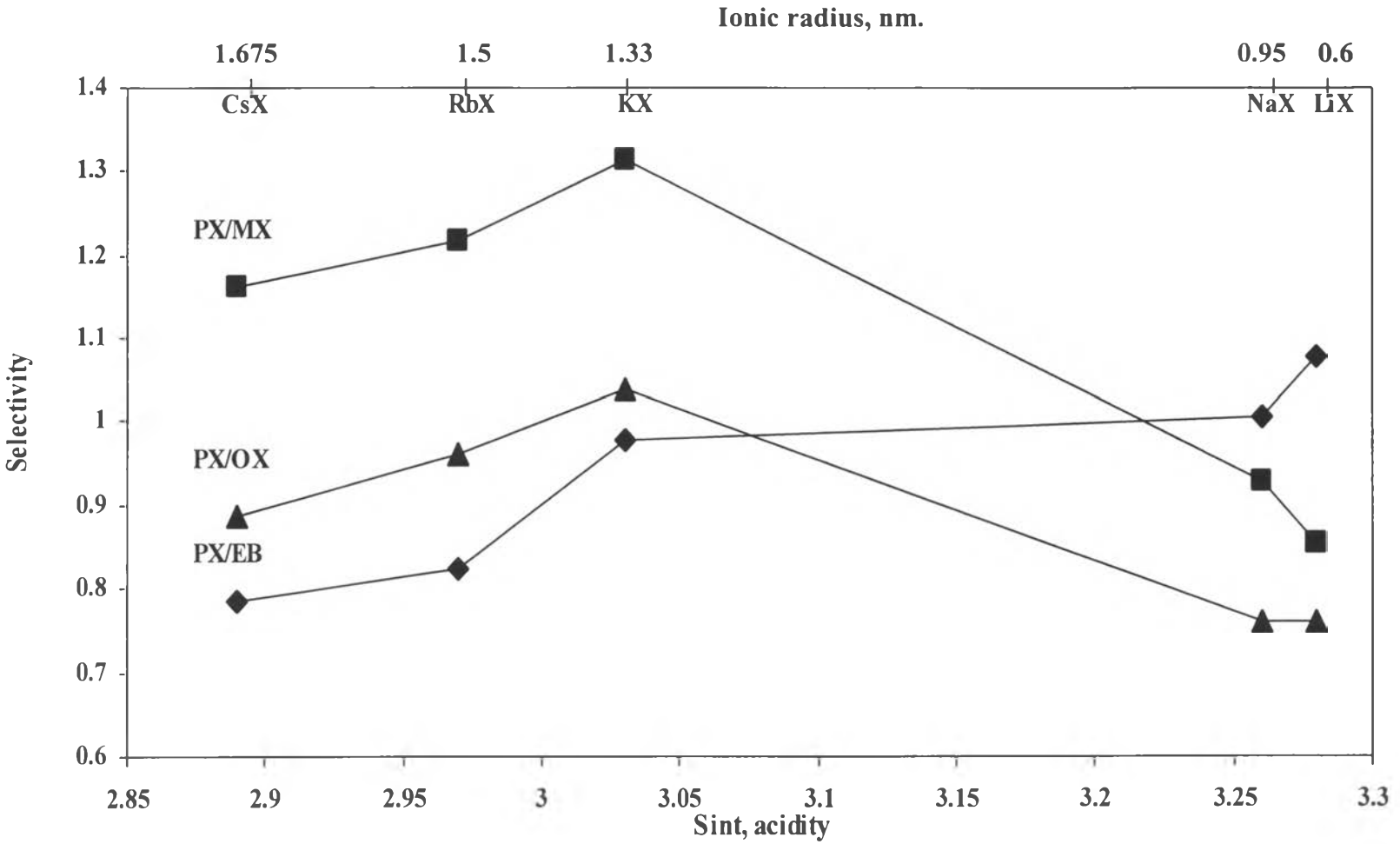

Figure 4.11 *PX* Selectivity VS Cationic radius and *X*-Zeolite acidity

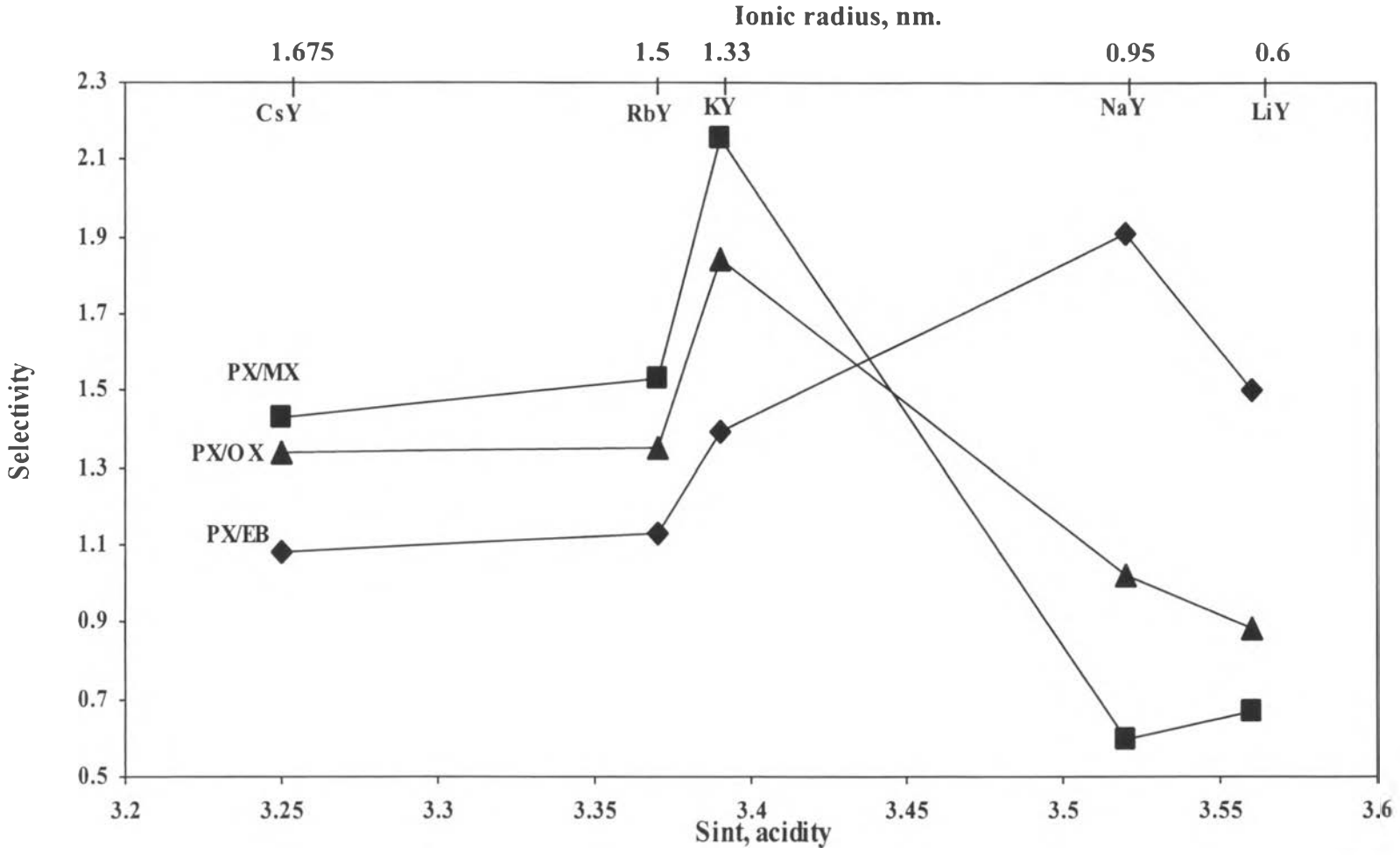

Figure 4.12 *PX* Selectivity VS Cationic radius and *Y*-Zeolite acidity

in the zeolite supercage is hindered sterically by *Cs* and *Rb*, which have larger ionic radii than *K*. However, with *Na* and *Li* exchanged zeolites, effect of the acid-base interaction dictates the *p*-xylene selectivity.

Nevertheless, different results were observed for the *p*-xylene selectivity with respect to ethylbenzene as seen in Figures 4.11 and 4.12. The selectivity increases from *Cs* to *Rb, K, Na* and *Li* exchanged *X* zeolites but slightly decreases from *Na* to *Li* exchanged *Y* zeolites. The explanations on the effects of the exchanged cations size and acid-base interaction are not valid in this case. Further study on this is needed to explain this phenomena.

Figure 4.13 shows the correlation plot between *p*-xylene selectivity and zeolite acidity of both *X* and *Y* zeolites. This plot confirms that only acid-base interaction can not be used to explain the adsorption mechanism for the whole range of the studied cations. Other effects such as exchanged cation size must be taken into account.

Effect of zeolite type is shown in Figure 4.14. Obviously, for the same exchanged cation, the *p*-xylene selectivity of the *Y* zeolites is higher than that of the *X* zeolites. However, the *p*-xylene selectivity with respect to *m*-xylene of *NaX* and *LiX* is higher than that of *NaY* and *LiY* because the high acidity of *p*-xylene, which is the weakest basicity, can be adsorbed less in the pore of *NaY* and *LiY*. On the other hand, *m*-xylene, the strongest basicity, can be adsorbed more. Interestingly, *KY* provides the high *p*-xylene selectivity. Therefore, additional study focusing on *KY* by using the breakthrough and adsorption isotherm techniques was carried out.

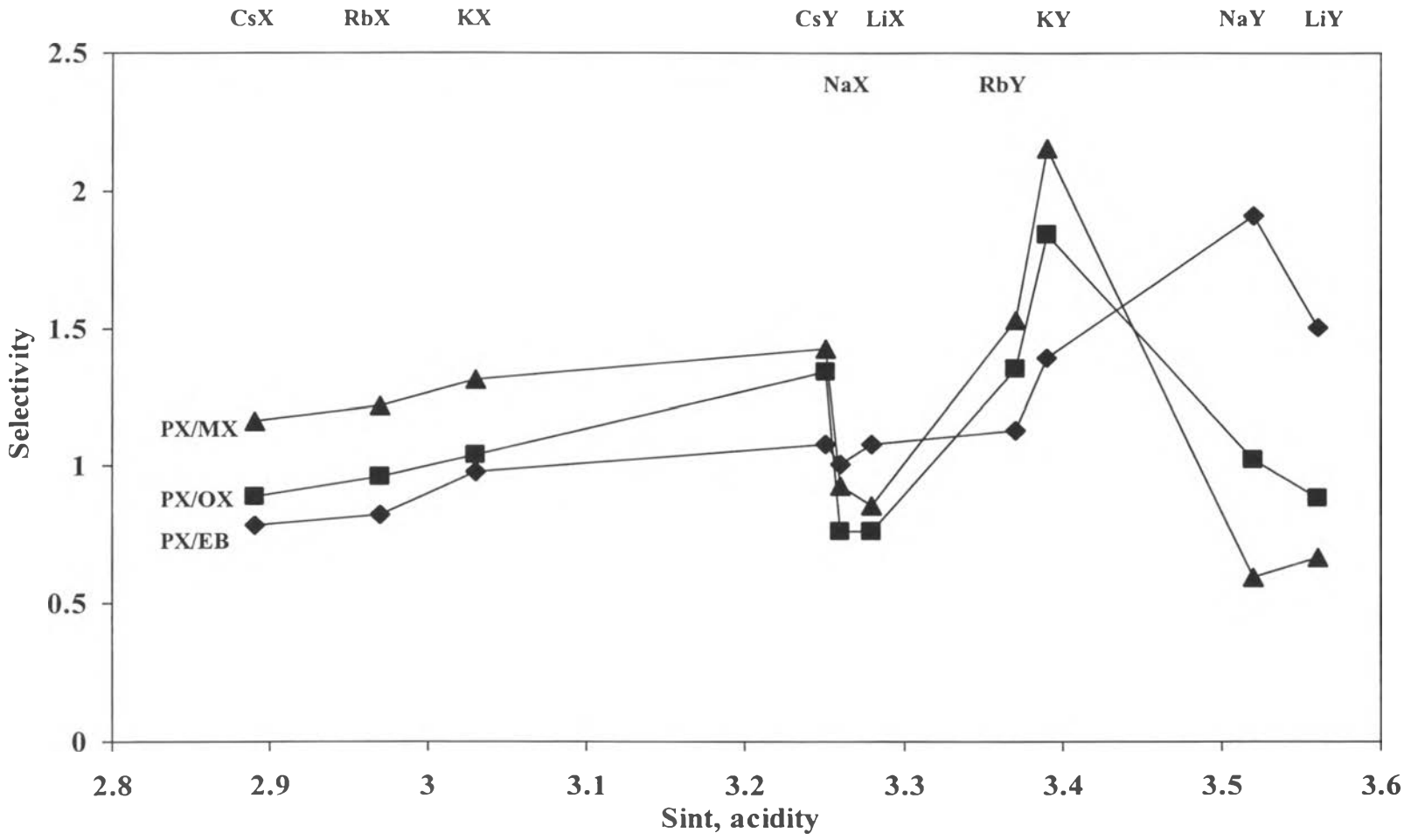

Figure 4.13 *PX* Selectivity VS Zeolite acidity

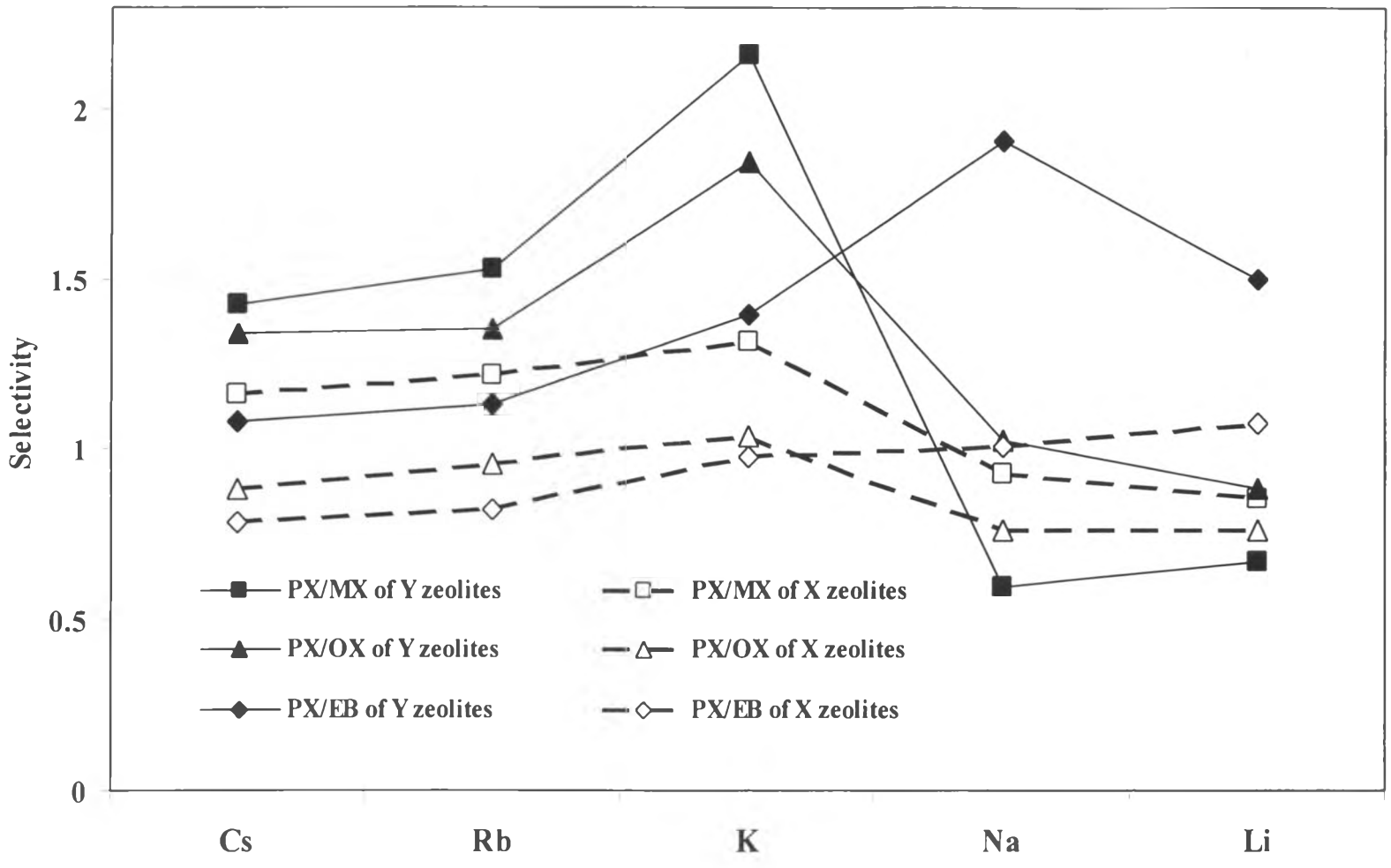

Figure 4.14 Effect of zeolite type

4.2 Dynamic Adsorption and Equilibrium Adsorption on *KY*

Figures 4.15-4.19 show the results from dynamic adsorption experiment. The plots can be interpreted in the same way as in the dynamic adsorption pulse test. Comparison results from the dynamic adsorption: breakthrough test (1) and equilibrium adsorption (2) are represented as a bar graph in Figure 4.20. For both methods, *KY* preferentially adsorbs *p*-xylene followed by ethylbenzene, *o*-xylene and *m*-xylene. Therefore, *p*-xylene selectivity with respect to *m*-xylene is higher than that to *o*-xylene and ethylbenzene, respectively. Furthermore, both methods provide comparable *p*-xylene selectivity. For example, on the first feed, the *p*-xylene selectivity with respect to *m*-xylene obtained from the breakthrough and autoclave tests are 2.7 and 2.93. The *p*-xylene selectivity with respect to *o*-xylene are 2.23 and 2.54 and the *p*-xylene selectivity with respect to ethylbenzene are 1.55 and 1.71. Therefore, it can be concluded that the two methods are exchangeable.

The results from Figure 4.20 also show that the *p*-xylene selectivity is not affected by the feed concentration. As the *p*-xylene concentration in feed increases, the *p*-xylene selectivity is approximately constant. That is also true with other species concentration that it does not affect the *p*-xylene selectivity as shown in Figures 4.21-4.23.

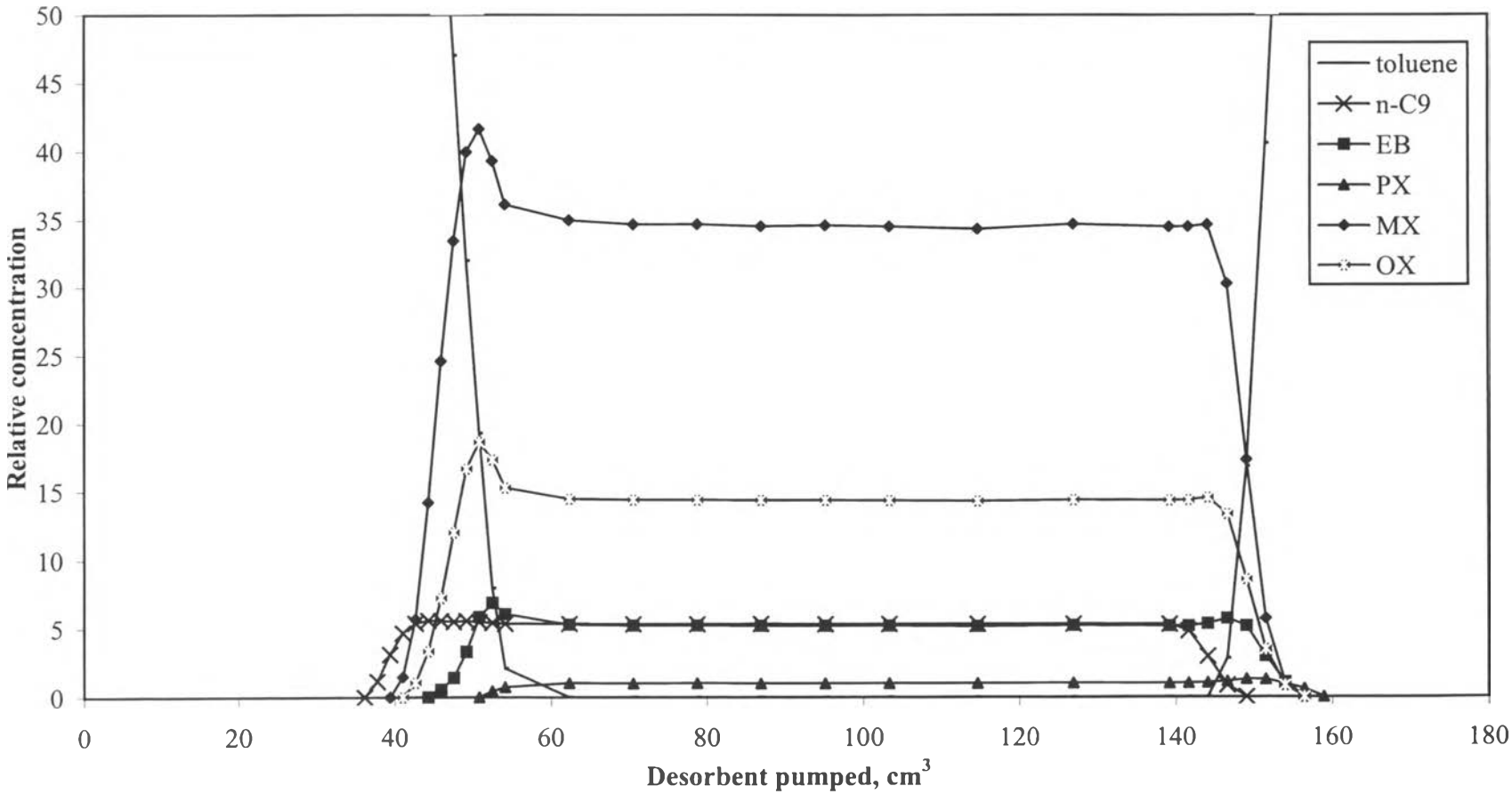

Figure 4.15 Dynamic adsorption: Breakthrough test, Blend 1

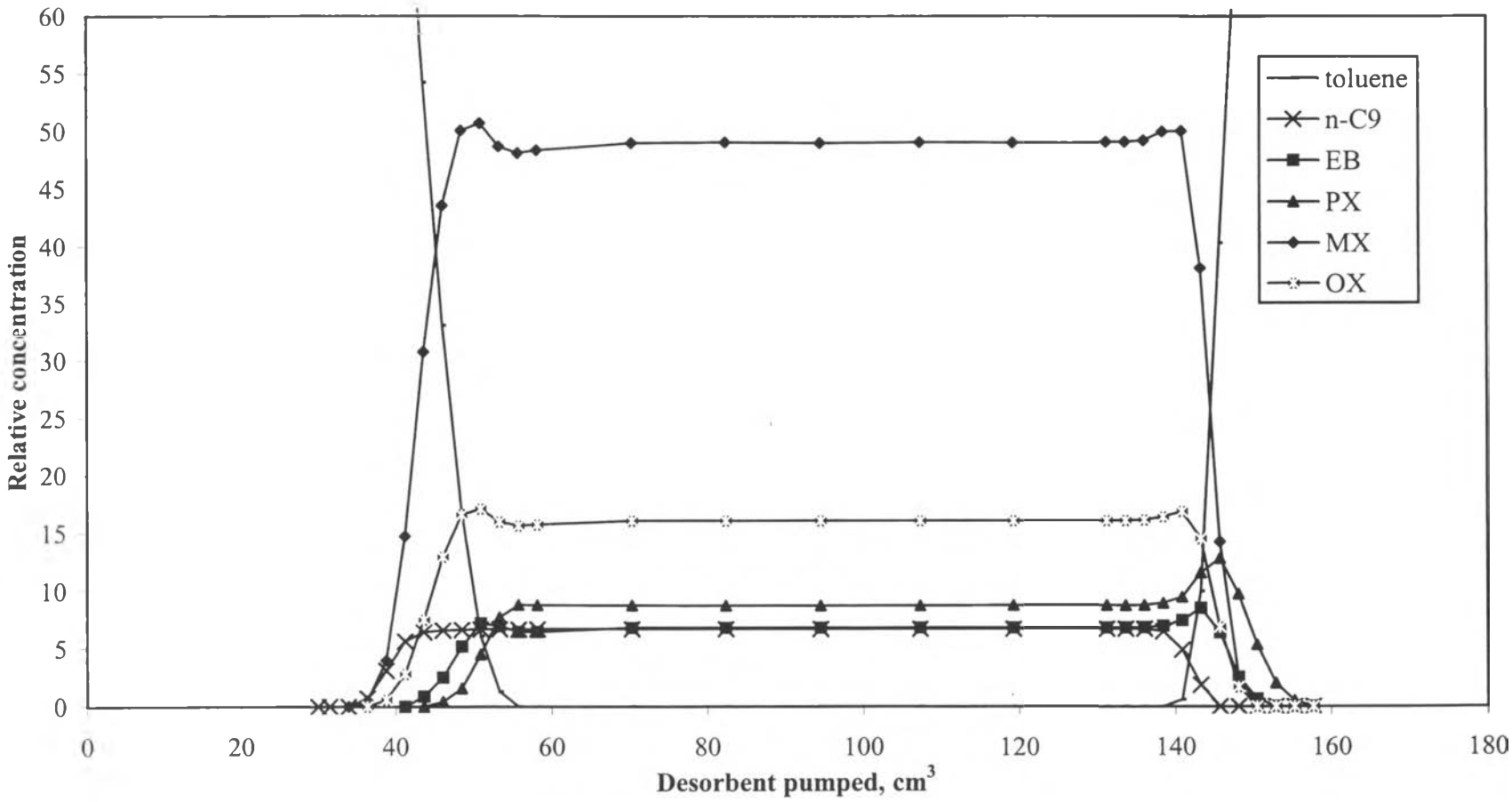

Figure 4.16 Dynamic adsorption: Breakthrough test, Blend 2

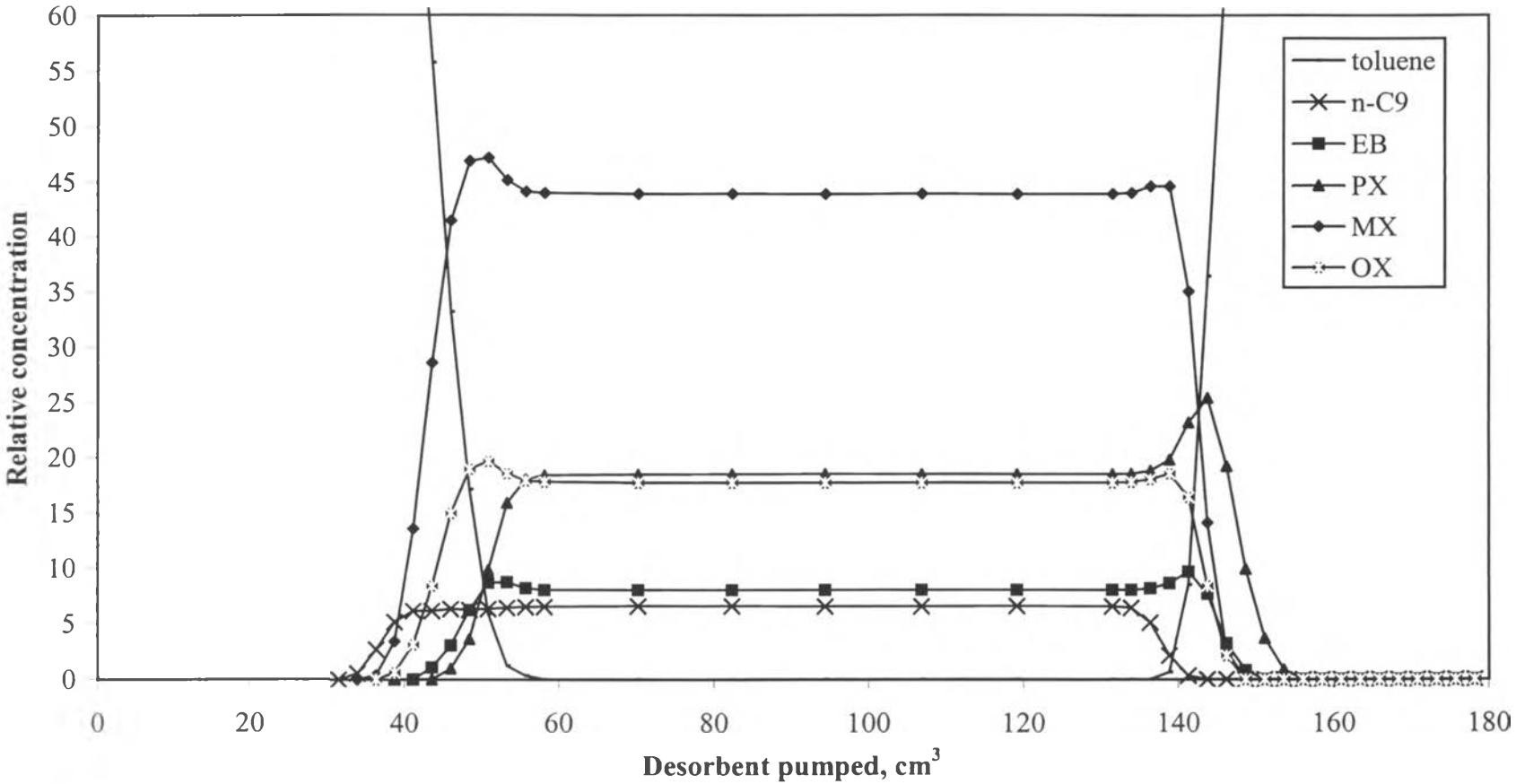

Figure 4.17 Dynamic adsorption: Breakthrough test, Blend 3

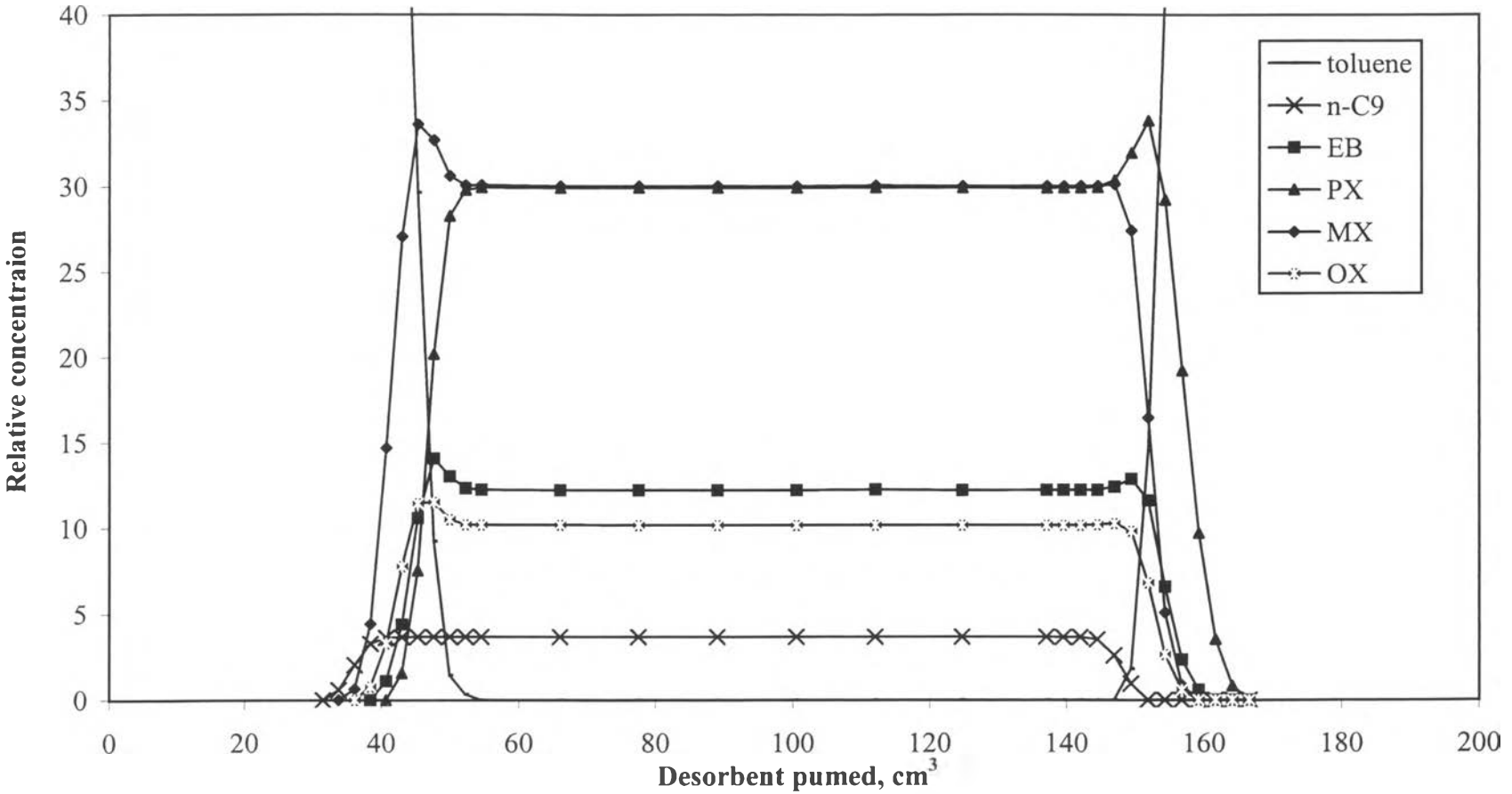

Figure 4.18 Dynamic adsorption: Breakthrough test, Blend 4

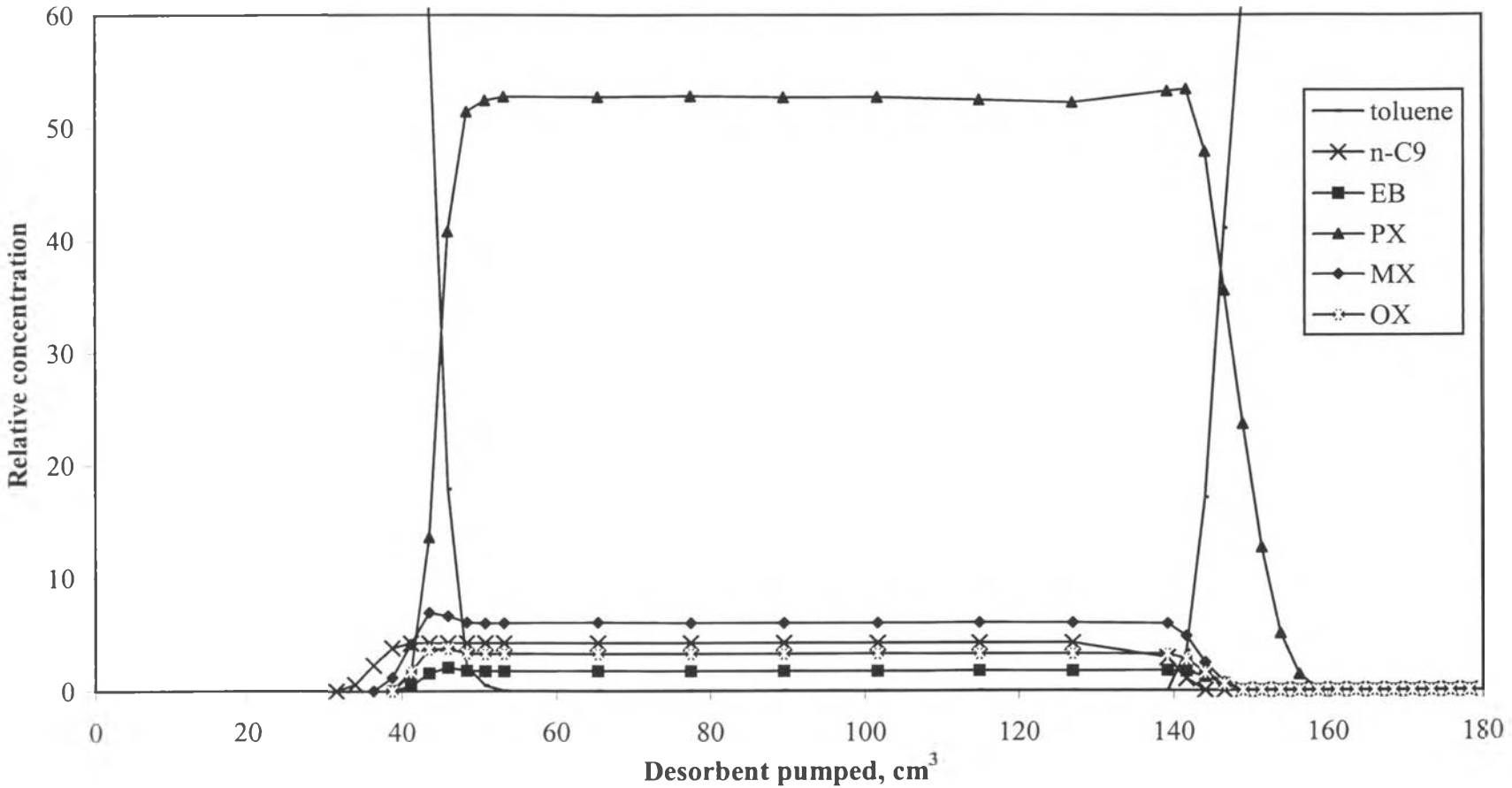

Figure 4.19 Dynamic adsorption: Breakthrough test, Blend 5

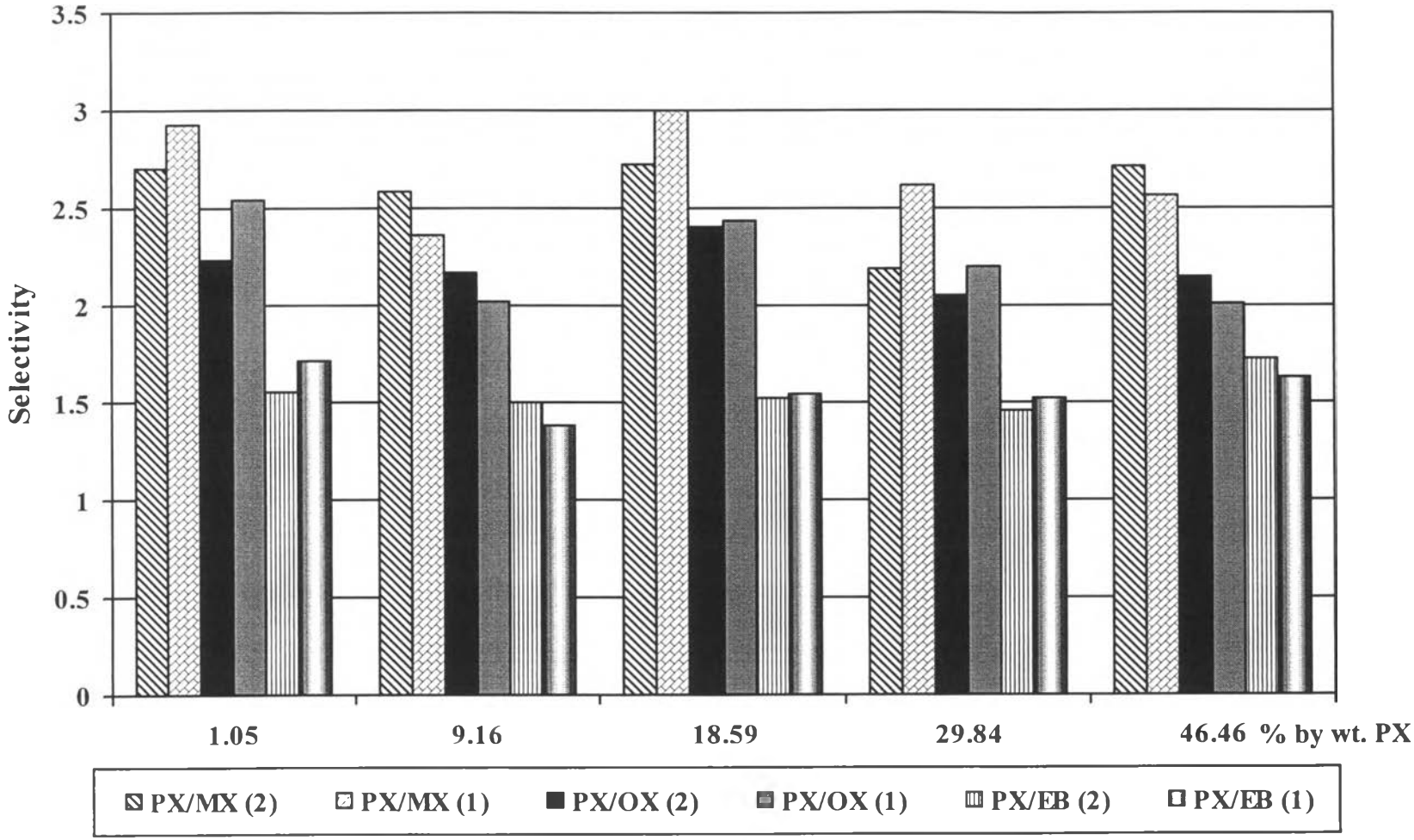

Figure 4.20 The comparison between the dynamic adsorption (1) and equilibrium adsorption (2)

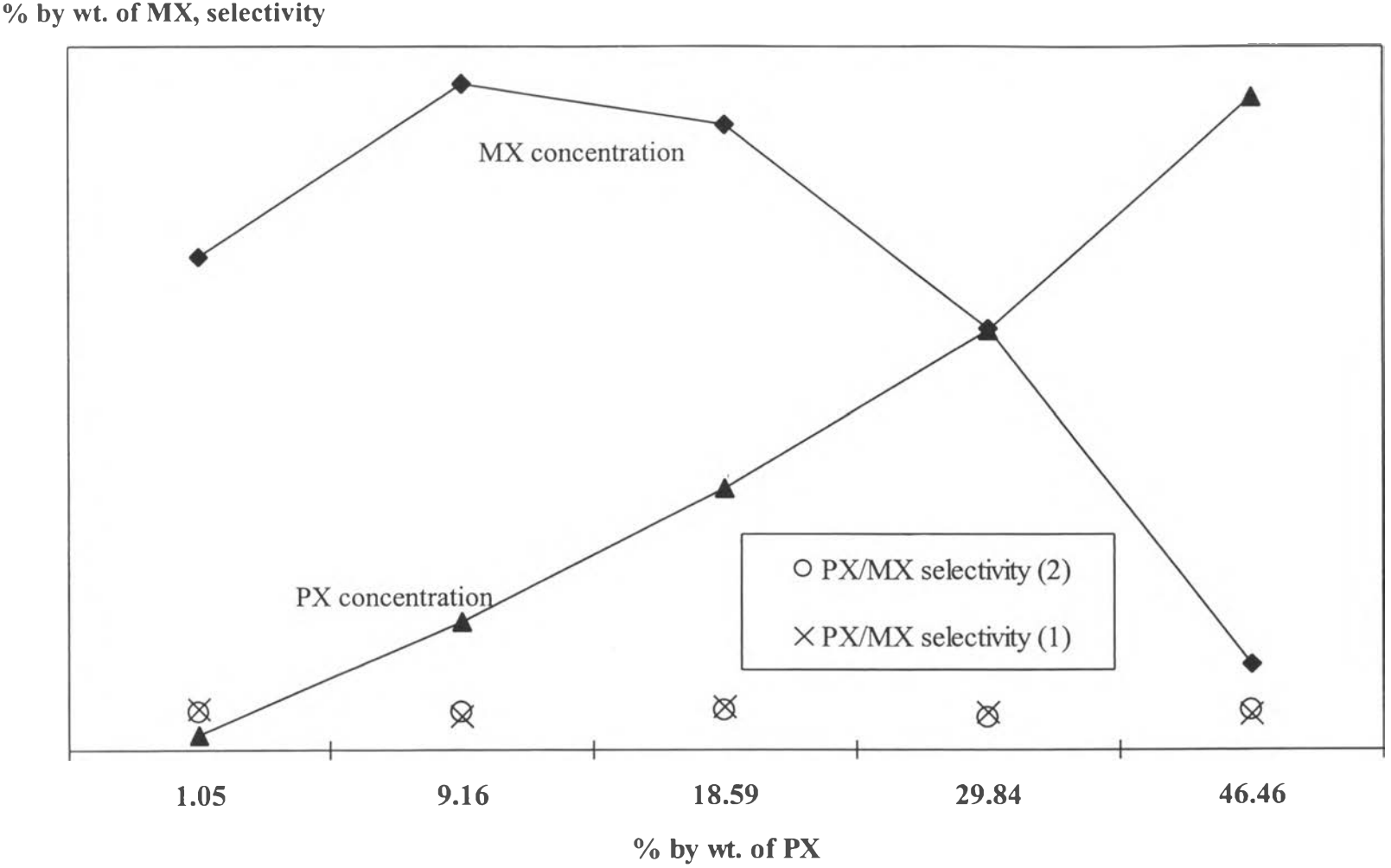

Figure 4.21 Effect of MX concentration to PX/MX selectivity

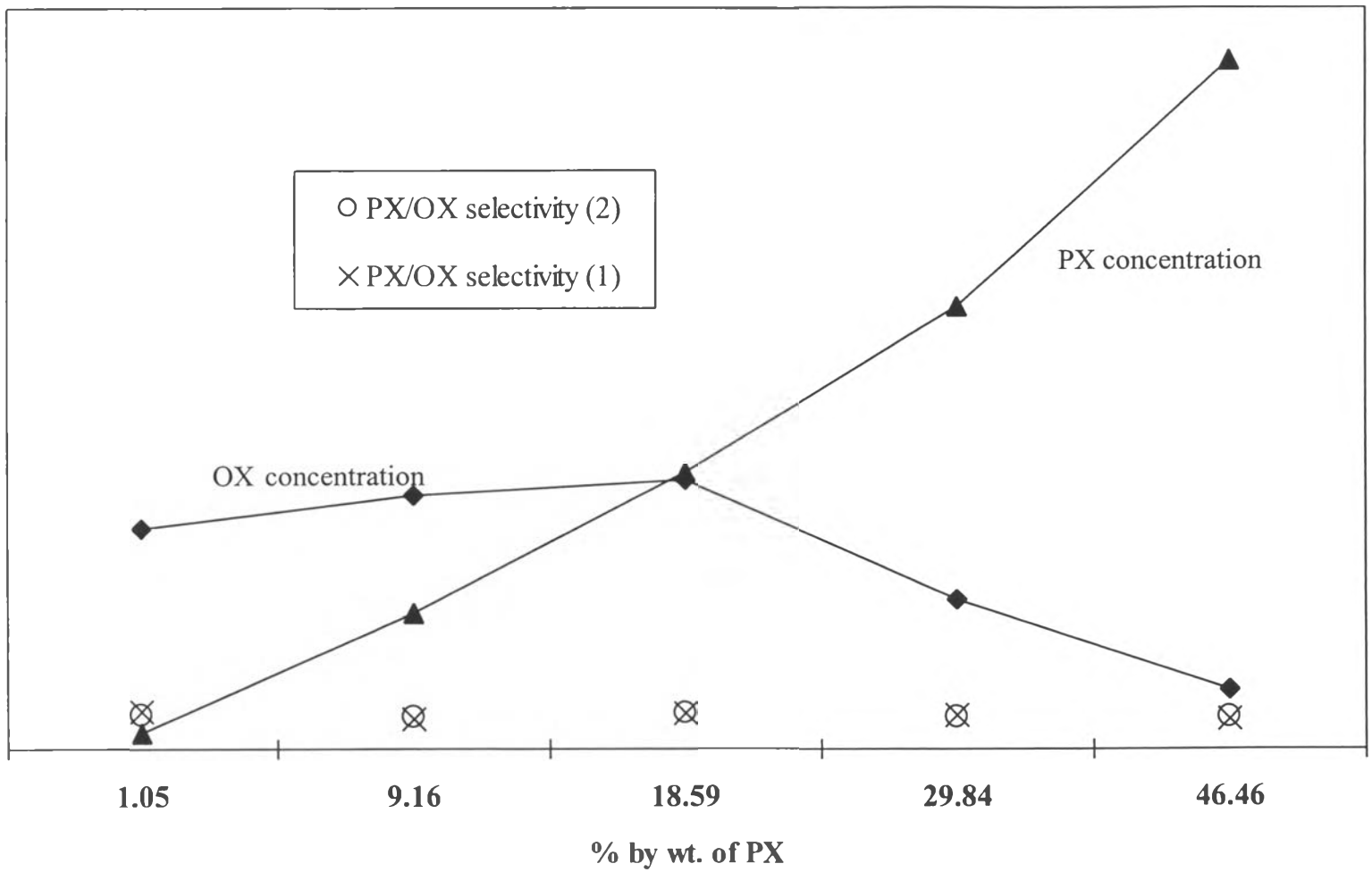

Figure 4.22 Effect of OX concentration to PX/OX selectivity

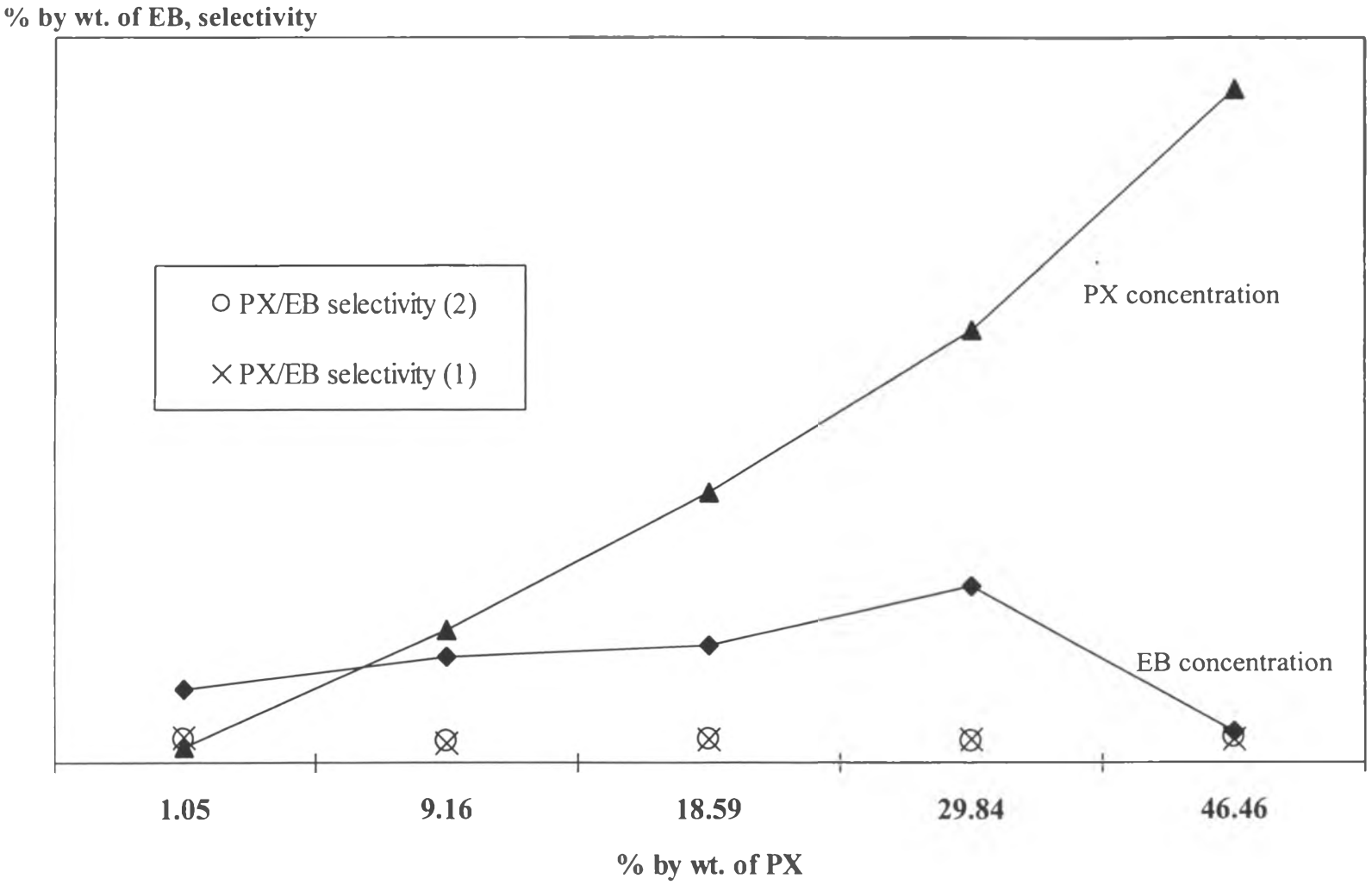

Figure 4.23 Effect of EB concentration to PX/EB selectivity

4.3 Heat of Adsorption of the C_8 Aromatics on *KY*

The data obtained from the equilibrium adsorption experiment were used to calculate the heat of adsorption of the C_8 aromatics on *KY*. According to equations (2.2) and (2.3), k_1, which is a function of temperature can be calculated and expressed as

$$k_1 = K_{01} \exp\left(\frac{-\Delta H_1}{RT}\right) \tag{4.1}$$

where K_{01} is the constant of species 1, ΔH_1 is the heat of adsorption of species 1 on the adsorbent, R is the gas constant, and T is the operating temperature. ΔH_1 and K_{01} are concentration and temperature independent parameters. Each calculation involved a set of data at different temperatures and concentrations. By using the Solver function in Microsoft Excel, k_1, K_{01} and ΔH_1 were calculated.

Varanyanond (2001) reported the heat of adsorption of each C_8 aromatics in the presence of toluene on *KY*. Comparison between ΔH from this work to those from Varanyanond (2001) is shown in Table 4.3.

Table 4.3 ΔH from Varanyanond (2001) and the present work

	Varanyanond (2001)	**This work**
component	ΔH, cal/g mole	ΔH, cal/g mole
PX	2.794	2.182
EB	1.784	1.444
OX	2.314	0.794
MX	1.784	0.732

The table shows that ΔH of *p*-xylene and ΔH of ethylbenzene from the previous work and the present work are comparable. It can be postulated that, for single component and multi-component adsorption, the adsorption mechanism of *p*-xylene and ethylbenzene on *KY* are similar. However, the considerable discrepancy

was found for *m*-xylene and *o*-xylene. The explanation on this phenomenon is still ambiguous. The presence of many components in the system might be attributed to the *m*-xylene and *o*-xylene adsorption mechanisms. Therefore, further study on this is needed.

ΔH calculated from this work shows the same trend as the adsorption order. That is ΔH of *p*-xylene is the highest followed by ethylbenzene, *o*-xylene and *m*-xylene, respectively. As *p*-xylene is adsorbed the most on the adsorbent, so the heat released from adsorption, heat of adsorption, would be the highest.